Physics Letters A 380 (2016) 822–827

Contents lists available at ScienceDirect

Physics Letters A

www.elsevier.com/locate/pla

Exciton-polariton wakefields in semiconductor microcavities

H. Terças [a,b,*], J.T. Mendonça [c,d]

[a] Physics of Information Group, Instituto de Telecomunicações, Lisbon, Portugal
[b] Institute for Theoretical Physics, University of Innsbruck, Technikerstrasse 25, 6020 Innsbruck, Austria
[c] Instituto de Física, Universidade de São Paulo, São Paulo SP, 05508-090 Brazil
[d] IPFN, Instituto Superior Técnico, 1049-001 Lisboa, Portugal

A R T I C L E I N F O

Article history:
Received 17 December 2015
Accepted 6 January 2016
Available online 21 January 2016
Communicated by F. Porcelli

Keywords:
Exciton-polaritons
Microcavities
Wakefields
Laser control
Strong coupling

A B S T R A C T

We consider the excitation of polariton wakefields due to a propagating light pulse in a semiconductor microcavity. We show that two kinds of wakes are possible, depending on the constituents fraction (either exciton or photon) of the polariton wavefunction. The nature of the wakefields (pure excitonic or polaritonic) can be controlled by changing the speed of propagation of the external pump. This process could be used as a diagnostic for the internal parameters of the microcavity.

1. Introduction

Semi-conductor microcavities, designed to increase the light-matter coupling, consist of a pair of distributed Bragg mirrors confining a electromagnetic mode and one (or several) quantum well with an exciton resonance [1,2]. In the strong coupling regime, where the exciton–photon coupling overcomes the losses, a new type of elementary excitations, called exciton polaritons (or cavity polariton), is formed [3]. Polaritons are therefore a coherent superposition of semi-conductor excitations (excitons) with light (photons).

One of the crucial aspects for the rapid development of research in the field of semi-conductor microcavities stems from the fact that polaritons may undergo Bose–Einstein condensation [4,5] – which has been experimentally observed in a series of works [6–12] –, putting together the fields of quantum optics and Bose–Einstein condensates (BEC) [13]. The most important differences with respect to the usual atomic BECs are: i) the possibility of condensation to occur at higher temperatures, as a consequence to the very small polariton mass (typically, $m \sim 10^{-5} m_e$) and ii) the fact of polariton BEC being a driven-dissipative phenomenon [14, 15], where the condensate is a steady state resulting from the pumping-loss balance. Nevertheless, it has also been shown that a thermodynamic regime for polariton condensates created by a nonresonant pump (i.e. pumped far away with respect to the condensation energy minimum) is possible, allowing for the definition of a temperature and a chemical potential for the system [16]. Another important property of polariton BECs concerns superfluidity. The phase transition expected for two-dimensional polaritons is a Berezinskii–Kosterlitz–Thouless (BKT) transition toward a superfluid state [17] and not a true BEC. Such a phase transition has not yet been observed in CdTe-based and GaN-based structures, as a consequence of a strong structural disorder leading to the formation of a glass phase [18] and to condensation in the potential minima of the disorder potential [19]. Signatures of BKT transition have nevertheless been reported in cleaner, GaAs-based samples [20]. Some interesting features related to the nonlinearity of the system, such as amplification [21] and optical bistability [22] have been investigated. Moreover, recent theoretical studies and experimental observation of topologically stable half-solitons [23–25] and half-vortices [26,27] in spinor polariton condensates have allowed the study of the dynamics and many-body properties of topological defects in the presence of external fields [28–30].

In the most usual experimental configurations, the external pump is fixed, occupying a well defined region of the planar cavity. However, if we allow the pump to move, the occurrence of new time-dependent phenomena can be expected in exciton-polaritons, even below the condensation threshold. Such an experimental configuration can be achieved with a pulsed laser, which propagation velocity can be controlled by changing the incidence angle [29]

* Corresponding author.
E-mail addresses: hugo.tercas@uibk.ac.at (H. Terças), titomend@ist.utl.pt (J.T. Mendonça).

http://dx.doi.org/10.1016/j.physleta.2016.01.024

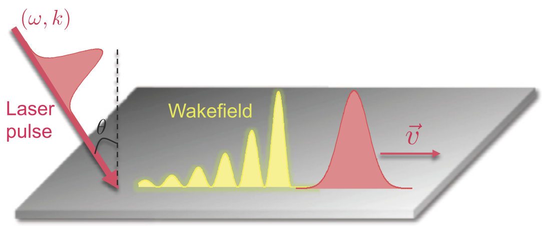

Fig. 1. (Color online.) Schematic representation of the experimental setup to produce wakefields. A laser pulse of frequency ω and momentum k is sent into the cavity (represented here by the shadowed rectangle). The velocity of the pulse is controlled with the incidence angle θ, such that $v = c\sin\theta$. The wakefield is behind the pulse.

(see Fig. 1 for a schematic representation). In this work, we study the properties wakefields in semi-conductor microcavities excited by a light pulse. Wakefields are universal phenomena which can be produced by the motion of a boat in the surface of a lake, or by a laser pulse propagating in a gas, having important technological implications in the case of laser-plasma acceleration [31]. When an intense electromagnetic pulse hits the plasma, it produces a wake of plasma oscillations through the action of a ponderomotive force. Electrons trapped in the wake can then be accelerated up to very high (relativistic) energies, providing an alternative yet efficient way of accelerating charged particles [32,33]. Acoustic wakefields produced by a Bose–Einstein condensate moving across a thermal (non-condensed) gas have also been considered [34,35]. Recently, wakefield excitation in metallic nanowires has also been investigated and pointed out as mechanism to produce energetic ultra-violet (XUV) radiaton [36]. In the present work, we show that a similar process can occur in a gas of excitons and exciton-polaritons (we should refer to the latter as "polaritons"), depending on the point of the dispersion that the system is pumped.

The structure of this paper is the following. In Section 2, we establish the basic equations of our problem. We start from the coupled photon–exciton wave equations and derive the energy spectrum. We then include the external pump term and derive the appropriate wakefield equations. In Section 3, we derive the wakefield solution for an exciton gas, by assuming that the lower polariton branch is pumped in the exciton-dominated part (high-wavevector). In Section 4, we derive the general form of polariton wakefields, produced if the pumped is tuned near the bottom of the polariton dispersion. Finally, in Section 5, we state some conclusions.

2. Basic equations

The coupled dynamics of the photonic and excitonic fields, respectively represented by $\phi(\mathbf{r},t)$ and $\chi(\mathbf{r},t)$, can be described by the following equations [1,37,38]

$$i\hbar\frac{\partial\phi}{\partial t} = -\left[\frac{\hbar^2}{2m_\phi}\nabla^2 + \frac{i\hbar}{2\tau_\phi}\right]\phi + \frac{\hbar}{2}\Omega_R\chi + P, \tag{1}$$

$$i\hbar\frac{\partial\chi}{\partial t} = -\left[\frac{\hbar^2}{2m_\chi}\nabla^2 + \frac{i\hbar}{2\tau_\chi}\right]\chi + \frac{\hbar}{2}\Omega_R\phi + \alpha_1|\chi|^2\chi, \tag{2}$$

where we have considered the special case of zero detuning between the laser and the cavity mode. Here, $m_\phi \ll m_e$ and $m_\chi \le m_e$ are the photon and exciton masses, respectively (m_e represents the electron mass), and Ω_R is the Rabi frequency measuring the strength of the coupling. The nonlinear term $\alpha_1 = 6E_b a_B^2/\mathcal{S}$, where $\mathcal{S}$ is the normalization surface, E_b is the exciton binding energy and a_B the corresponding Borh radius, accounts for the polariton–polariton contact interactions [39]. Here, we choose the parameters according to the typical experimental conditions, $m_\phi = 5\times10^{-5}m_e$, $m_\chi = 0.4m_e$ and $\hbar\Omega_R = 8$ meV. The quantities τ_ϕ and τ_χ are the lifetimes of cavity photons and excitons, with typical values $\tau_\phi = 10$ ps and $\tau_\chi = 400$ ps.

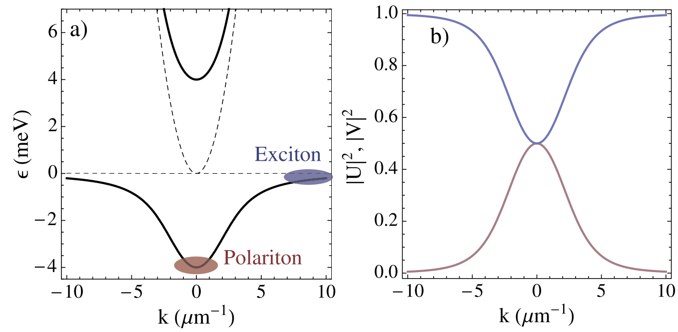

Fig. 2. (Color online.) Panel a): Lower and upper polariton branches in a semiconductor microcavity. We excite different wavevector ranges in the lower branch to generate the wake fields. Panel b): The Hopfield coefficients measuring the exciton ($|\mathcal{U}|^2$, upper curve) and photon ($|\mathcal{V}|^2$, lower curve) fractions. We have used typical parameters for a GaAs microcavity: $m_\phi = 5\times10^{-5}m_e$, $m_\chi = 0.4m_e$, and $\hbar\Omega_R = 8$ meV.

In Eq. (1), $P \equiv P(\mathbf{r},t)$ is the external pump, acting as a source of photons, which we choose to be resonantly tuned with respect to the lower polariton branch, as we specify below. We start by deriving the appropriate dispersion relations from the photon–exciton coupled field. The bare photonic and excitonic modes are readily obtained by neglecting the Rabi coupling Ω_R and the interaction term α_1,

$$i\hbar\frac{\partial\phi}{\partial t} = -\left[\frac{\hbar^2}{2m_\phi}\nabla^2 + \frac{i\hbar}{2\tau_\phi}\right]\phi, \tag{3}$$

$$i\hbar\frac{\partial\chi}{\partial t} = -\left[\frac{\hbar^2}{2m_\chi}\nabla^2 + \frac{i\hbar}{2\tau_\chi}\right]\chi, \tag{4}$$

for which we can find solutions of the form

$$\phi(\mathbf{r},t) = \phi_0\exp(i\mathbf{k}\cdot\mathbf{r} - i\omega_\phi t),$$
$$\chi(\mathbf{r},t) = \chi_0\exp(i\mathbf{k}\cdot\mathbf{r} - i\omega_\chi t). \tag{5}$$

Replacing in Eqs. (3)–(4), we obtain the dispersion relations

$$\omega_\phi = \frac{\hbar k^2}{2m_\phi} - i\gamma_\phi, \quad \omega_\chi = \frac{\hbar k^2}{2m_\chi} - i\gamma_\chi, \tag{6}$$

where the damping rates are given by $\gamma_\phi = 1/2\tau_\phi$ and $\gamma_\chi = 1/2\tau_\chi$. For a given value of the wavenumber k, we have $\omega_\phi \gg \omega_\chi$, as a result of the mass difference $m_\phi \ll m_\chi$. The polariton modes can then be obtained for a finite value of the Rabi field. Using again solutions of the form

$$(\phi,\chi)(\mathbf{r},t) = (\phi_0,\chi_0)\exp(i\mathbf{k}\cdot\mathbf{r} - i\omega t), \tag{7}$$

we can then derive the dispersion equation

$$(\omega-\omega_\phi)(\omega-\omega_\chi) = \frac{\tilde{\Omega}_R^2}{4}, \tag{8}$$

where $\tilde{\Omega}_R^2 = \Omega_R^2 - 4\gamma_\phi\gamma_\chi$ and ω_ϕ and ω_χ are determined by Eq. (6). Solving for ω, we get the two solutions $\omega_\pm$, such that

$$\omega_\pm = \frac{1}{2}\left[(\omega_\phi+\omega_\chi) \pm \sqrt{(\omega_\phi+\omega_\chi)^2 - 4\omega_\phi\omega_\chi + \tilde{\Omega}_R^2}\right]. \tag{9}$$

This corresponds to the lower (ω_-) and upper (ω_+) polariton branches, as illustrated in Fig. 2. The upper (U) and lower (L) polariton modes are given by $\psi_U = \mathcal{U}\chi + \mathcal{V}\phi$ and $\psi_L = \mathcal{V}\chi - \mathcal{U}\phi$, where the Hopfield coefficients, satisfying the normalization condition $|\mathcal{U}|^2 + |\mathcal{V}|^2 = 1$, are explicitly defined as

$$|\mathcal{U}|^2 = \frac{\omega_+\omega_\chi - \omega_-\omega_\phi}{(\omega_\phi + \omega_\chi)\sqrt{\Delta^2 + 4\Omega_R^2}}, \tag{10}$$

$$|\mathcal{V}|^2 = \frac{\omega_+\omega_\phi - \omega_-\omega_\chi}{(\omega_\phi + \omega_\chi)\sqrt{\Delta^2 + 4\Omega_R^2}}, \tag{11}$$

where $\Delta = \omega_\phi - \omega_\chi$. Near $k = 0$, the polariton is composed by 50% photon and 50% exciton (for the case of zero detuning $\delta \equiv \Delta|_{k=0} = 0$), while for higher values of $k \gg 0$, the excitonic fraction is much higher than the photonic one. Thus, the strategy to produce different kinds of wakefields consists in moving the pump with different velocities, corresponding to different points in the lower polariton brunch (see Fig. 2).

Let us now introduce a finite pump $P \neq 0$, while keeping the interaction term negligible. This can be done if the pump intensity is lower than the bistability threshold [40]. We further assume that the pump moves with constant velocity v along some direction z, and assume it to be uniform in the perpendicular direction, which allows us to write $P(\mathbf{r}, t) \equiv P(x - vt)$. By performing the following variable transformation $(x, t) \to (\xi, \tau)$, with $\xi = (x - vt)$, $\tau = t$, we can rewrite the exciton–photon field equations in terms of the Lagrangian variable ξ as

$$\left(\frac{\partial^2}{\partial\xi^2} - i\kappa_\phi\frac{\partial}{\partial\xi} + i\Gamma_\phi\right)\phi = \epsilon_\phi\chi + I(\xi), \tag{12}$$

$$\left(\frac{\partial^2}{\partial\xi^2} - i\kappa_\chi\frac{\partial}{\partial\xi} + i\Gamma_\chi - \alpha\,|\chi|^2\right)\chi = \epsilon_\chi\phi, \tag{13}$$

where we have introduced the new quantities

$$\kappa_\phi = \frac{2m_\phi}{\hbar}v, \quad \Gamma_\phi = \frac{2m_\phi}{\hbar}\gamma_\chi, \quad \epsilon_\phi = \frac{m_\phi}{\hbar}\Omega_R, \tag{14}$$

and

$$\kappa_\chi = \kappa_\phi\frac{m_\chi}{m_\phi}, \quad \Gamma_\chi = \Gamma_\phi\frac{m_\chi}{m_\phi}\frac{\tau_\phi}{\tau_\chi}, \quad \epsilon_\chi = \epsilon_\phi\frac{m_\chi}{m_\phi}, \tag{15}$$

with the new source term $I(\xi)$ and nonlinear parameter α defined as

$$I(\xi) = \frac{2m_\phi}{\hbar^2}P(\xi), \quad \alpha = \frac{2m_\chi}{\hbar}\alpha_1. \tag{16}$$

Eqs. (12)–(13) are the basic equations for the description of wakefields produced by the source $I(\xi)$ and are derived by assuming the quasi-static approximation, i.e. $\partial/\partial\tau = 0$. Such an approximation can be justified when the dispersion of the pulse is negligible, in a way that its shape $I(\xi)$ stays unchanged (which is the case for an externally applied pump propagating along short distances).

3. Exciton wakefields

In what follows, we consider the situation where the excitonic fraction of polaritons is much larger than the photon one. This corresponds to a large wavevector, $k \gg 0$, corresponding to a pump propagating with velocity $v \sim \hbar k/m_\chi$, as depicted in Fig. 2 (blue shadowed region). In this case, we can assume a local photon field solution of the form $i\Gamma_\phi\phi = I(\xi)$, and reduce the above two coupled equations to a single equation for the driven exciton field,

$$\left(\frac{\partial^2}{\partial\xi^2} - i\kappa_\chi\frac{\partial}{\partial\xi} + i\Gamma_\chi - \alpha\,|\chi|^2\right)\chi = -i\frac{\epsilon_\chi}{\Gamma_\chi}I(\xi). \tag{17}$$

Let us now define new variables such that

$$\chi(\xi) = h(\xi)\exp\left(\frac{i}{2}\kappa_\chi\xi\right), \tag{18}$$

where $h(\xi)$ is the exciton field envelope. Replacing in Eq. (17), we write

$$\left[\frac{\partial^2}{\partial\xi^2} + \kappa^2(\xi)\right]h = J(\xi), \tag{19}$$

where $\kappa(\xi)$ is a slowly varying function of the coordinate ξ, as given by

$$\kappa^2(\xi) = \frac{\kappa_\chi^2}{4} + i\Gamma_\chi - \alpha|h(\xi)|^2. \tag{20}$$

The exciton wakefield Eq. (19) describes a driven nonlinear oscillator. For causality reasons, the forced solution is such that the signal $h(\xi)$ must vanish upstream to the source $I(\xi)$, i.e. $h(\xi) = 0$ for $\xi > 0$. In that case, the formal solution for the exciton wavefunction envelope reads

$$h(\xi) = \int_\infty^\xi J(\xi')\sin\left[\varphi(\xi) - \varphi(\xi')\right]d\xi', \tag{21}$$

with the phase function $\varphi(\xi)$ defined as

$$\varphi(\xi) = \int^\xi \kappa(\xi')d\xi'. \tag{22}$$

Using the expression in Eq. (20), and assuming that the term in κ_χ is dominant, which corresponds to weakly damped and low amplitude wakefields, such that $\kappa_\chi^2 \gg \Gamma_\chi$ and $\kappa_\chi^2 \gg \alpha|h(\xi)|^2$, we get

$$\varphi(\xi) \simeq \frac{1}{2}\left(\kappa_\chi + 2i\frac{\Gamma_\chi}{\kappa_\chi}\right)\xi - \frac{2\alpha}{\kappa_\chi}\int^\xi |h(\xi')|^2 d\xi'. \tag{23}$$

In the linear case (i.e., below the bistability threshold [40]), when we can assume that $\alpha \simeq 0$, the wakefield solution (21) reduces to

$$h(\xi) = \int_\infty^\xi J(\xi')\sin\left[\frac{\kappa_\chi}{2}\left(1 + 2i\frac{\Gamma_\chi}{\kappa_\chi^2}\right)(\xi - \xi')\right]d\xi'. \tag{24}$$

These solutions are illustrated in Fig. 3. As we can observe, the wakefield amplitude decreases downstream, as a consequence of the finite life-time of excitons. Moreover, the amplitude of the wake decreases with the width σ_0 of the laser. The latter behavior can be understood from Eq. (24), giving the wakefield as a convolution between two functions: the larger the pulse, the stronger the interaction between the different modes of the Green function. More pronounced wakes are obtained for $J(\xi) = \delta(\xi)$.

4. Polariton wakefields

Let us now consider that the pump is tuned to be resonant with the bottom of the lower polariton branch, as illustrated in Fig. 2. In that case, the excitonic and the photonic fractions are nearly equal. We go back to Eqs. (12)–(13) and define the new field variables $g(\xi)$ and $h(\xi)$,

$$\phi(\xi) = g(\xi)\exp\left(\frac{i}{2}\kappa_\phi\xi\right), \quad \chi(\xi) = h(\xi)\exp\left(\frac{i}{2}\kappa_\chi\xi\right). \tag{25}$$

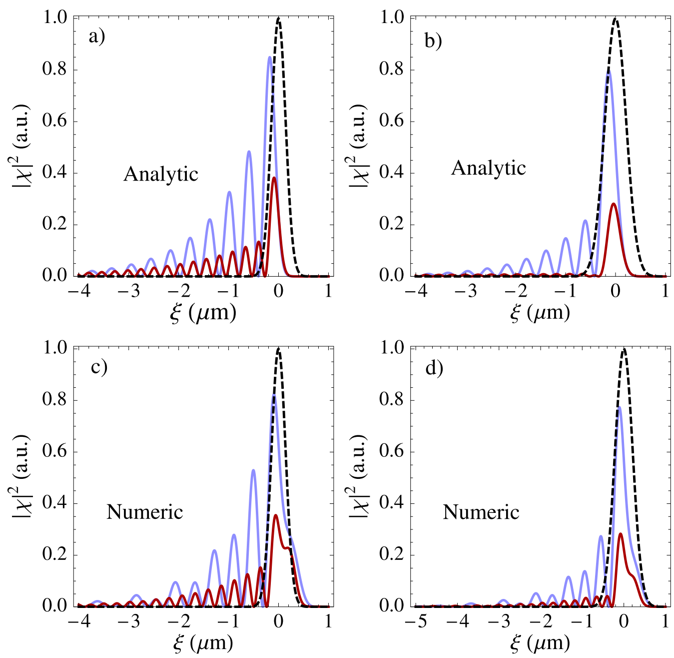

Fig. 3. (Color online.) Exciton wakefield produced by an external pulse propagating with velocity $v = 1.2$ nm/ps (blue/light gray lines, corresponding to $\kappa_\chi = 8.4\ \mu\text{m}^{-1}$) and $v = 1.8$ nm/ps (red/dark gray lines, corresponding to $\kappa_\chi = 12\ \mu\text{m}^{-1}$). Panels a) and b) are the analytic solutions obtained from Eq. (24), while panels b) and d) depict the numerical solutions obtained from Eq. (17). We have used $\sigma_0 = 0.2\ \mu$m for the panels a) and c) (resp. $\sigma_0 = 0.4\ \mu$m for the panels b) and d)). In all situations, we have normalized the wakefield amplitude relatively to the pump intensity I_0 and used the following parameters [1,40]: $m_\phi = 5 \times 10^{-5} m_e$, $m_\chi = 0.4 m_e$, $\tau_\phi = 30$ ps, $\tau_\chi = 400$ ps and $\hbar\Omega_R = 8$ meV.

Replacing in the coupled wakefield equations, we get

$$D_\phi^2 g \equiv \left(\frac{\partial^2}{\partial \xi^2} + \kappa_\phi^2\right) g = a_\phi h + I(\xi) e^{-i\kappa_\phi \xi/2}, \tag{26}$$

$$D_\chi^2 h \equiv \left[\frac{\partial^2}{\partial \xi^2} + \kappa_\chi^2(\xi)\right] h = a_\chi g, \tag{27}$$

with the new quantities

$$\kappa_\phi'^2 = \frac{\kappa_\phi^2}{4} + i\Gamma_\phi, \quad \kappa_\chi'^2(\xi) = \frac{\kappa_\chi^2}{4} + i\Gamma_\chi - \alpha |h(\xi)|^2, \tag{28}$$

and

$$a_\phi = \epsilon_\phi e^{i(\kappa_\chi - \kappa_\phi)\xi/2}, \quad a_\chi = \epsilon_\chi e^{-i(\kappa_\chi - \kappa_\phi)\xi/2}. \tag{29}$$

We can derive a closed equation for the exciton envelope $h(\xi)$ from Eqs. (26)–(27), which can be written as

$$D_\phi^2 D_\chi^2 h = \frac{\partial^2 \ln a_\chi}{\partial \chi^2} D_\chi^2 h + a_\phi a_\chi h + a_\chi I(\xi) e^{-i\kappa_\phi \xi/2}. \tag{30}$$

Rearranging the terms, one can finally obtain

$$\left(\frac{\partial^4}{\partial \xi^4} + \kappa_a^2 \frac{\partial^2}{\partial \xi^2} + \kappa_b^4\right) h = J'(\xi), \tag{31}$$

where we have used $J' = a_\chi I(\xi) \exp(-i\kappa_\phi \xi/2)$ and

$$\kappa_a^2 = \kappa_\phi^2 + \kappa_\chi^2 + (\kappa_\chi - \kappa_\phi)^2/4,$$
$$\kappa_b^4 = \kappa_\phi^2 \kappa_\chi^2 + (\kappa_\chi - \kappa_\phi)^2 \kappa_\phi^2/4 - \epsilon_\phi \epsilon_\chi. \tag{32}$$

Eq. (31) is the polariton wakefield equation, which includes both the exciton and the photon dynamics. This equation can be solved

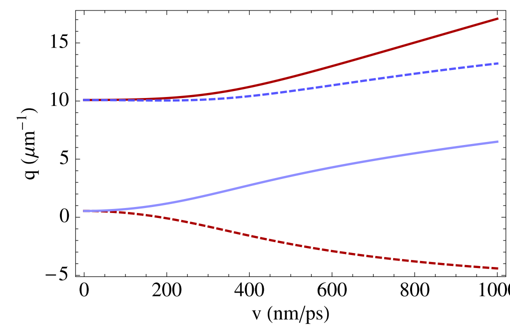

Fig. 4. (Color online.) Wakefield wave vectors q_- (blue/light gray) and q_+ (red/dark gray) as a function of the pulse velocity v. The solid (dashed) lines represents the real (imaginary) parts of q_- and q_+. We observe that the fast mode q_+ is less damped.

with the Green's function method. We take the Fourier transform of the latter to obtain

$$h(q) = J'(q) G(q'), \tag{33}$$

where $h(q)$ and $J'(q)$ are the Fourier components of the functions $h(\xi)$ and $J'(\xi)$, as defined by

$$h(\xi) = \int h(q) e^{iq\xi} \frac{dq}{2\pi}, \quad J'(\xi) = \int J'(q) e^{iq\xi} \frac{dq}{2\pi}, \tag{34}$$

and $G(q)$ is the Fourier transformed Green's function,

$$G(q) = \frac{1}{(q^4 - q^2 \kappa_a^2 + \kappa_b^4)}. \tag{35}$$

Applying the convolution theorem, we can write the wakefield solution to Eq. (31) as

$$h(\xi) = \int_{-\infty}^{\infty} J'(\xi) G(\xi - \xi') d\xi', \tag{36}$$

where $G(\xi)$ is the inverse Fourier transform of $G(q)$. We then get the following solution

$$h(\xi) = \frac{2}{\kappa_a^2} \int_{-\infty}^{\infty} \left\{ \frac{1}{q_+} \sin[q_+(\xi - \xi')] - \frac{1}{q_-} \sin[q_-(\xi - \xi')] \right\} H(\xi - \xi') J'(\xi') d\xi'. \tag{37}$$

Here, $H(\xi)$ is the Heaviside function and $q_\pm$ are the two poles of Eq. (35),

$$q_\pm^2 = \frac{1}{2}\kappa_a^2 \left(1 \pm \sqrt{1 - 4\frac{\kappa_b^4}{\kappa_a^4}}\right), \tag{38}$$

which can also be written as

$$q_\pm^2 = \frac{1}{2}\kappa^2 \left(1 \pm \sqrt{1 - 4\frac{\epsilon_\phi \epsilon_\chi}{\kappa^4}}\right),$$
$$\kappa^2 = \kappa_\phi^2 + \kappa_\chi^2 + (\kappa_\chi - \kappa_\phi)^2/4. \tag{39}$$

The slow and fast wake modes $q_\pm$ are separated by one order of magnitude, as shown in Fig. 4. Similarly to the case of excitonic wakes described in the previous section, finite exciton (and in the present case also photon) lifetime leads to wake damping, which is related to the imaginary of the modes $q_\pm$.

In order to illustrate the physical meaning of the wakefield solution (37), we determine the wake left behind a Gaussian pump

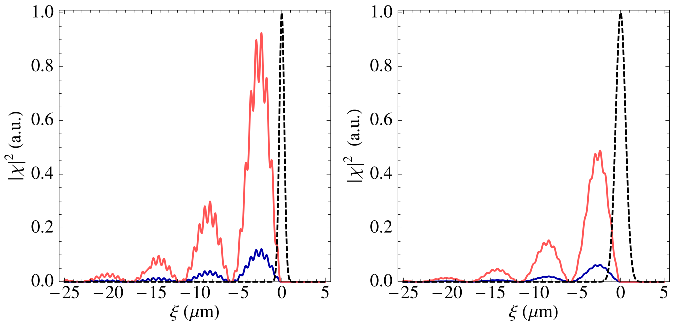

Fig. 5. (Color online.) Numerical example of a polariton wakefield, produced by a moving external source, corresponding to the following parameters: $m_\phi = 5 \times 10^{-5} m_e$, $m_\chi = 0.4 m_e$, $\tau_\phi = 30$ ps, $\tau_\chi = 400$ ps and $\hbar\Omega_R = 10$ meV. The red/light gray lines are obtained for $v = 0.1$ nm/ps, while the blue/darker lines correspond to $v = 0.08$ nm/ps. In the left (right) panel, we used $\sigma_0 = 0.1$ µm ($\sigma_0 = 0.3$ µm). We have used the same cavity parameters as in Fig. 2.

$I(\xi) = I_0 \exp(-\xi^2/\sigma_0^2)$, where σ_0 is the beam width and $I_0 = (2m_\phi/\hbar^2)P_0$ is the maximum external pump intensity. The source term in (37) is then given by

$$J(\xi) = I_0 \epsilon_\chi e^{-i\kappa_\chi \xi/2} \exp\left(-\frac{\xi^2}{\sigma_0^2}\right). \quad (40)$$

The polariton wakefield solution is illustrated in Fig. 5. We can clearly identify two different oscillations, one determined by the exciton-like dynamics, which is similar to the one shown in Fig. 4 (fast modulation), and a second one determined by the photon-like dynamics (slow modulation). We also observe that the fast modulation, which possess smaller amplitude, is less damped that the slow mode (see Fig. 4). This is so because the exciton lifetime is much larger than the photon mode. We notice that the slow and fast oscillations propagate with the same phase velocity, which equals the velocity v of the moving source. Such a synchronism between the velocity of the moving object and the phase velocity of the wakefield oscillations is a characteristic features of the wakefields [31,36]: a pulse moving with group velocity v is in resonance with the modes of phase velocity ω_L/k and the wake contains only those modes. This is of course true for nondispersive wakefields, produced by narrow light pulses, which corresponds to our case. One interesting application of wakefields in practical experiments can be the acceleration of excitons, in the same way that neutral atoms are accelerated in laser-plasma wakefields [41]: although excitons (or polaritons) cannot be accelerate by an electric field, as they are neutral particles, electrons and holes alone can. One then may think of combining the electron–hole plasma acceleration with the electron–hole recombination effect, designing a scheme to produce energetic beams of excitons or exciton-polaritons. We reserve the study of exciton acceleration to a future work. Exciton-polariton wakefields can also be used as an alternative way of characterizing microcavities, as the form of the wake is strictly related on the basic properties of the semi-conductor and the cavity (quality factor, exciton and photon lifetimes, coupling strength, etc). The access to time-resolved spectra, with the aid of a streak camera, may allow direct and very accurate measurements of wakefield features (modulation frequencies, amplitude and damping rate).

5. Conclusions

We have investigated the generation of wakefields in a semi-conductor microcavity in the strong coupling regime excited by a moving external pump source. This opens the way to the study of non-stationary regimes in driven-dissipative cavities, which could lead to further theoretical studies and could also stimulate a new type of time-resolved experimental observations. We have shown that the nature of the wake, being either purely excitonic or polaritonic, can be controlled by tuning the pump wavevector. While in the former case the wakefield corresponds to a single frequency modulation of the exciton wavefunction envelope, in the latter the wakefield consists of a two-frequency modulation. The fast (slow) mode is associated with the excitonic (photonic) fraction of the polariton fluid. The influence of the transverse shape of the moving source, the relation of the resulting wakefields, the possible Cherenkov emission and the polariton acceleration will be left to a future work.

Acknowledgements

H. Terças thanks the support from Fundação para a Ciência e a Tecnologia (Portugal), namely through programs PTDC/POPH and projects UID/Multi/00491/2013, UID/EEA/50008/2013, IT/QuSim and CRUP-CPU/CQVibes, partially funded by EU FEDER, and from the EU FP7 projects LANDAUER (GA 318287) and PAPETS (GA 323901).

References

[1] I.A. Shelykh, A.V. Kavokin, Yu.G. Rubo, T.C.H. Liew, G. Malpuech, Semicond. Sci. Technol. 25 (2010) 013001.
[2] I. Carusotto, C. Ciuti, Rev. Mod. Phys. 85 (2013) 299.
[3] J.J. Hopfield, Phys. Rev. 112 (1958) 1555.
[4] G. Malpuech, Y.G. Rubo, F.P. Laussy, P. Bigenwald, A.V. Kavokin, Semicond. Sci. Technol. 18 (2003) S395.
[5] M. Zamfirescu, A. Kavokin, B. Gil, G. Malpuech, M. Kaliteevski, Phys. Rev. B 65 (2002) 161205(R).
[6] J. Kasprzak, M. Richard, S. Kundermann, A. Baas, P. Jeambrun, J.M.J. Keeling, F.M. Marchetti, M.H. Szymanska, R. Andre, J.L. Staehli, V. Savona, P.B. Littlewood, B. Deveaud, Le Si Dang, Nature 443 (2006) 409.
[7] M. Richard, J. Kasprzak, R. Andre, R. Romestain, L.S. Dang, G. Malpuech, A. Kavokin, Phys. Rev. B 72 (2005) 201301(R).
[8] R. Balili, V. Hartwell, D. Snoke, L. Pfeiffer, K. West, Science 316 (2007) 1007.
[9] S. Utsunomiya, L. Tian, G. Roumpos, C.W. Lai, N. Kumada, T. Fujisawa, M. Kuwata-Gonokami, A. Loffler, S. Hofling, A. Forchel, Y. Yamamoto, Nat. Phys. 4 (2008) 700.
[10] J.J. Baumberg, A.V. Kavokin, S. Christopoulos, A.J.D. Grundy, R. Butte, G. Christmann, D.D. Solnyshkov, G. Malpuech, G. Baldassarri Hoger von Hogersthal, E. Feltin, J.-F. Carlin, N. Grandjean, Phys. Rev. Lett. 101 (2008) 136409.
[11] J. Kasprzak, D.D. Solnyshkov, R. Andre, Le Si Dang, G. Malpuech, Phys. Rev. Lett. 101 (2008) 146404.
[12] E. Wertz, L. Ferrier, Dmitry D. Solnyshkov, P. Senellart, D. Bajoni, A. Miard, A. Lemaitre, G. Malpuech, J. Bloch, Appl. Phys. Lett. 95 (2009) 051108.
[13] L. Pitaevskii, S. Stringari, Bose–Einstein Condensation, Oxford Science Publications, 2003.
[14] M. Wouters, I. Carusotto, Phys. Rev. Lett. 99 (2007) 140472.
[15] A. Chiocchetta, I. Carusotto, Europhys. Lett. 102 (2013) 67007.
[16] H. Deng, et al., Phys. Rev. Lett. 97 (2006) 146402.
[17] G. Malpuech, Y.G. Rubo, F.P. Laussy, P. Bigenwald, A. Kavokin, in: J.J. Baumberg, L. Viña (Eds.), Special Issue on Microcavities, Semicond. Sci. Technol. 18 (2003) S395.
[18] G. Malpuech, D.D. Solnyshkov, H. Ouerdane, M.M. Glazov, I. Shelykh, Phys. Rev. Lett. 98 (2007) 206402.
[19] D. Sanvitto, A. Amo, L. Vina, R. Andre, D. Solnyshkov, G. Malpuech, Phys. Rev. B 80 (2009) 045301.
[20] C.W. Lai, N.Y. Kim, S. Utsunomiya, G. Roumpos, H. Deng, M.D. Fraser, T. Byrnes, P. Recher, N. Kumada, T. Fujisawa, Y. Yamamoto, Nature 450 (2007) 529.
[21] P.G. Savidis, et al., Phys. Rev. Lett. 84 (2000) 1547.
[22] A. Baas, et al., Phys. Rev. B 70 (2004) 161307.
[23] H. Flayac, I.A. Shelykh, D.D. Solnyshkov, G. Malpuech, Phys. Rev. B 81 (2010) 045318.
[24] D.D. Solnyshkov, H. Flayac, G. Malpuech, Phys. Rev. B 85 (2012) 073105.
[25] R. Hivet, H. Flayac, D.D. Solnyshkov, D. Tanese, T. Boulier, D. Andreoli, E. Giacobino, J. Bloch, A. Bramati, G. Malpuech, A. Amo, Nat. Phys. 8 (2012) 724.
[26] Yu.G. Rubo, Phys. Rev. Lett. 99 (2007) 106401.
[27] F. Manni, T.C.H. Liew, K.G. Lagoudakis, C. Ouellet-Plamondon, R. André, V. Savona, B. Deveaud, Phys. Rev. B 88 (2013) 201303(R).
[28] H. Terças, D.D. Solnyshkov, G. Malpuech, Phys. Rev. Lett. 110 (2013) 035303.
[29] H. Terças, H. Flayac, D.D. Solnyshkov, G. Malpuech, Phys. Rev. Lett. 112 (2014) 066402.
[30] H. Terças, D.D. Sonlyshkov, G. Malpuech, Phys. Rev. Lett. 113 (2014) 036403.

[31] T. Tajima, J.M. Dawson, Phys. Rev. Lett. 43 (1979) 267.
[32] R. Bingham, J.T. Mendonça, P.K. Shukla, Plasma Phys. Control. Fusion 46 (2004) R1.
[33] J.T. Mendonça, Theory of Photon Acceleration, Institute of Physics Publ., Bristol, 2001.
[34] J.T. Mendonça, P.K. Shukla, R. Bingham, Phys. Lett. A 340 (2005) 355.
[35] J.T. Mendonça, H. Terças, Physics of the Ultra-Cold Matter, Springer Ser. Opt. At. Plasma Phys., Springer-Verlag, NY, 2013.
[36] S. Ali, H. Terças, J.T. Mendonça, Phys. Rev. B 83 (2011) 153401.
[37] I.A. Shelykh, Y.G. Rubo, G. Malpuech, D.D. Solnyshkov, A. Kavokin, Phys. Rev. Lett. 97 (2006) 066402.
[38] H. Flayac, D.D. Solnyshkov, G. Malpuech, Phys. Rev. B 83 (2011) 045412.
[39] C. Ciuti, V. Savona, C. Piermarocchi, A. Quattropani, P. Schwendimann, Phys. Rev. B 58 (1998) 7926.
[40] A. Kavokin, J. Baumberg, G. Malpuech, F. Laussy, Microcavities, Oxford University Press, 2007.
[41] R. Rajeev, T. Madhu Trivikram, K.P.M. Rishad, V. Narayanan, E. Krishnakumar, M. Krishnamurthy, Nat. Phys. 9 (2013) 185.